

Low-dielectric, nanoporous polyimide films prepared from PEO–POSS nanoparticles

Yuan-Jyh Lee^a, Jieh-Ming Huang^b, Shiao-Wei Kuo^a, Feng-Chih Chang^{a,*}

^a*Institute of Applied Chemistry, National Chiao-Tung University, Hsin-Chu, Taiwan, ROC*

^b*Department of Chemical Engineering, Van Nung University, Chung-Li, Taiwan, ROC*

Received 25 March 2005; received in revised form 21 July 2005; accepted 16 August 2005

Available online 29 August 2005

Abstract

Dielectric insulator materials that have low dielectric constants ($k < 2.5$) are required as inter-level dielectrics to replace silicon dioxide (SiO_2) in future semiconductor devices. In this paper, we describe a novel method for preparing nanoporous polyimide films through the use of a hybrid PEO–POSS template. We generated these nanoporous foams by blending polyimide as the major phase with a minor phase consisting of the thermally labile PEO–POSS nanoparticles. The labile PEO–POSS nanoparticles would undergo oxidative thermolysis to release small molecules as byproducts that diffuse out of the matrix to leave voids into the polymer matrix. We achieved significant reductions in dielectric constant (from $k = 3.25$ to 2.25) for the porous PI hybrid films, which had pore sizes in the range of 10–40 nm.

© 2005 Elsevier Ltd. All rights reserved.

Keywords: Low- k materials; Nanoparticles; Polyimide

1. Introduction

As integrated circuit (IC) dimensions continue to decrease, device performances do not necessarily decrease accordingly because of the substantial increases in interconnect delays, cross-talk noise, and power dissipation [1–3]. Materials that possess with low dielectric (low- k) constants are being developed to replace silicon dioxide (SiO_2 , $k > 3.5$) as the inter-level dielectric. Recently, the specifications for insulating films are that their dielectric constants should be ca. 3.0 and, within the next generation of IC production, devices may require materials to have dielectric constants approaching or below 2.0 [4,5]. Because most solid materials have relatively high dielectric constants ($k > 3$), one way of preparing low- k materials from them is to introduce voids into their film to take advantage of the lowest dielectric constant of air ($k = 1$). Such nanoporous and mesoporous materials have attracted a tremendous

amount of interest for use in IC devices for microelectronics technologies [6–10].

Although many types of porous materials have been explored in recent years, few meet the stringent requirements for low- k materials ($k < 2.2$), namely, good thermal stability, low moisture uptake, and high mechanical strength. The greatest limitation on a material's qualification for device application is its behavior toward the stringent IC processing conditions: It must be thermally and chemically stable and resistant to chemical and mechanical treatments [11,12]. Currently studies on porous materials have been based on two general routes: One is the thermal decomposition of polymer blends or by block copolymers, the other is through blending of a highly thermal stable polymer [6–8] with an unstable one [9,10]. For example, Carter et al. developed a highly fluorinated polyimide with low dielectric constants ($k < 2.3$) by using the nanofoam approach [7]. Unfortunately, fluorinated polymers have inadequate thermal stability for use in current integration procedures, and there are concerns for fluorine evolution during processing and its reactions with the metals used [13–15]. Therefore, a number of reports [6–8] have described the synthesis of porous structures of high-temperature thermoplastic materials ($T_g > 350^\circ\text{C}$) from

* Corresponding author. Tel.: +886 3 5727077; fax: +886 3 5719507.
E-mail address: changfc@mail.nctu.edu.tw (F.-C. Chang).

block copolymers. Block copolymers are good candidates for templates because their structures are microphase-separated into nanoscale domains. These block copolymers are usually consisting of a highly temperature-stable block and a thermally labile block, which acts as the dispersed phase through the curing process. Pore formation can be accomplished by thermolysis of the labile blocks, which leaves pores of sizes and shapes that correspond to those present in the initial copolymer's morphology. The ultimate dielectric constant achievable is limited primarily due to two factors [16,17]: The intrinsic dielectric constant of the matrix and the sizes of the dispersion pores in the materials. The introduction of nanometer-sized pores into these materials is a natural extension of this strategy to increase the amount of free space. Matrixes containing homogeneous, nanometer-scaled, and closed pores are preferred in terms of their electrical and mechanical properties. The effect that the porosity has on the dielectric constant can be predicted using simple models, such as the Bruggeman effective medium approximation [18]:

$$f_1 \frac{k_1 + k_e}{k_1 + 2k_e} + f_2 \frac{k_2 - k_e}{k_2 + 2k_e} = 0$$

where f_1 and f_2 represent the fractions of the two components, k_1 and k_2 are the dielectric constants of the components, and k_e is the effective dielectric constant of the material. This model assumes that the material has two components: The matrix of the solid and its pores. This approach has been adopted generally for the development of porous low- k materials. When the porosity exceeds 30%, these pores will become percolated or interconnected. The percolated channels in the low- k material give rise to a number of reliability concerns, such as the local trapping of moisture and chemicals, which leads to an increase in dielectric constant, and crack formation.

In this paper, we present a new method for preparing the nanoporous polyimide film through the use of hybrid poly(ethylene oxide)–polyhedral oligosilsesquioxane (PEO–POSS) nanoparticles as templates. For the polymer matrix, we used a common polyimide derived from pyromellitic dianhydride (PMDA) and oxydianiline (ODA). In this study, we have grafted oligomeric poly(ethylene oxide) (PEO) chains ($M_w = 200$ g/mol) onto POSS and the PEO–POSS nanoparticles were then blended with the PMDA–ODA polyamic acid (PAA) prior to its thermal imidization reaction. This hybrid consists of a highly temperature-stable polyimide ($T_g = 370$ °C) and thermally labile PEO–POSS nanoparticles ($T_d = 250$ °C, in air). The labile PEO–POSS nanoparticles behave as the dispersed phase through a thermal oxidative degradative mechanism. POSS has a well-defined structure with a Si_8O_{12} silsesquioxane core (0.5 nm) and eight organic functional group or hydrogen atoms (R or H) presented on the silicon atoms [19–23]. Functionalization of POSS can be achieved by the hydrosilylation reactions of the Si–H groups

present on the silsesquioxane core (T_8^{H} or $\text{Q}_8\text{M}_8^{\text{H}}$) in the presence of a platinum catalyst. The route were followed to produce PEO–POSS was to react $\text{Q}_8\text{M}_8^{\text{H}}$ POSS with allyl-terminated PEO (allyl-PEO) using a Pt–dvs complex as catalyst. Using this hybrid material, we explored the possibility of incorporating porous moieties into a polyimide matrix to create films of low dielectric constant, high thermal stability, and good dynamic mechanical strength.

2. Experimental

2.1. Materials

Mono-hydroxyl-terminated poly(ethylene oxide) oligomer (PEO, average molecular weight 200), allyl bromide, *N,N'*-dimethylacetamide (DMAc), and the platinum complex (Pt–dvs, 2 wt% Pt in xylene) were purchased from Aldrich, USA. The solution of the platinum complex was diluted 100-fold with xylene prior to use. Toluene was dried by distillation before use in the hydrosilylation reaction. The POSS derivative ($\text{Q}_8\text{M}_8^{\text{H}}$) was purchased from the Hybrid Plastics Co., USA. Ultrapure pyromellitic dianhydride (PMDA) and 4,4'-oxydianiline (ODA) were purchased from the Chriskev Inc., USA.

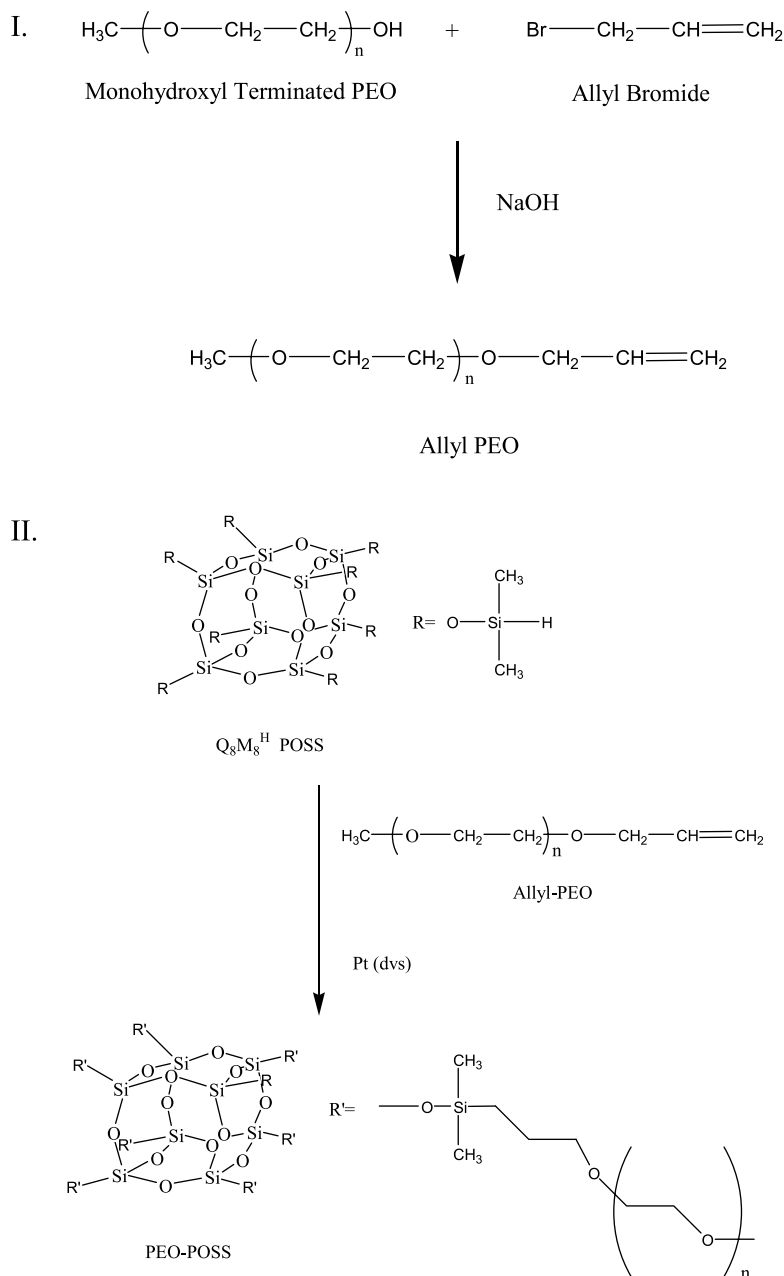
2.2. Syntheses

2.2.1. The vinyl-terminated PEO (allyl-PEO) and the PEO-functionalized silsesquioxane (PEO–POSS)

The allyl-terminated PEO (allyl-PEO) was prepared according to the procedure presented in Scheme 1: The reaction of mono-hydroxyl-terminated group polymer with a large excess of allyl bromide in the bulk at 70 °C for 24 h in the presence of NaOH solution ($[\text{NaOH}/\text{OH groups}] = 2$). After filtration and evaporation of the unreacted allyl bromide, the functionalized oligomer (allyl-PEO, molecular weight 240) was dried under high vacuum at 60 °C. The functionalized POSS derivative bearing eight PEO chains (PEO–POSS) was synthesized from the reaction (Scheme 1) of octa-silane-functionalized POSS ($\text{Q}_8\text{M}_8^{\text{H}}$) with the allyl-terminated PEO (allyl-PEO). Typically, allyl-PEO (2.4 g, 10 mmol) and $\text{Q}_8\text{M}_8^{\text{H}}$ POSS (1.02 g, 1 mmol) were dissolved in dry toluene (20 mL) and then a solution of Pt complex (Pt–dvs, 0.1 mL, 200 ppm) was injected into the solution using a syringe. The solution was then heated at 80 °C with stirring under nitrogen until the Si–H peak (2200 cm^{-1}) totally disappeared completely (12 h). The solvent and unreacted allyl-PEO were evaporated under vacuum at 120 °C. The resulting product, PEO–POSS, was obtained as a viscous yellow liquid (3.42 g).

2.2.2. Preparation of polymer hybrids with porous structure

ODA (6.50 g, 32.5 mmol) and DMAc (58.23 mL) were added to a three-necked flask equipped with a mechanical stirrer, and cooled in an ice-water bath under a nitrogen



Scheme 1. Reaction scheme for preparing the PEO-functionalized POSS nanoparticles.

atmosphere. After the ODA had dissolved completely, PMDA (7.08 g, 32.5 mmol) was added and the mixture was stirred at room temperature for 12 h. At this point, PEO-POSS (0.75 g, 5 wt%) was added into the flask and the mixture was stirred for 30 min at room temperature. The obtained DMAc solution of the polyamic acid/PEO-POSS was coated with a doctor blade onto a glass plate using an automatic film applicator at a rate of 0.34 mm/min, and, subsequently, the plate were heated at 60, 80, 100, 150, 200, 250 and 300 °C under a nitrogen atmosphere. The film was then peeled off from the glass plate to obtain the polyimide/POSS hybrid film (thickness: 200 μm), which was used for tests of the material's dielectric and

mechanical properties. Using this general approach, a series of hybrids having PEO-POSS compositions of 0, 2, 5 and 10 wt% were prepared. The PEO-POSS component was decomposed by heating the films at 250 °C for 12 h, and then annealing at 280 °C for 4 h in air to yield the porous polyimide films.

2.3. Characterizations

^1H nuclear magnetic resonance (^1H NMR) spectra were obtained at 300 MHz using a Bruker DPX-300 spectrometer. Fourier transform infrared (FT-IR) spectroscopy measurements were performed using a Nicolet Avatar 320

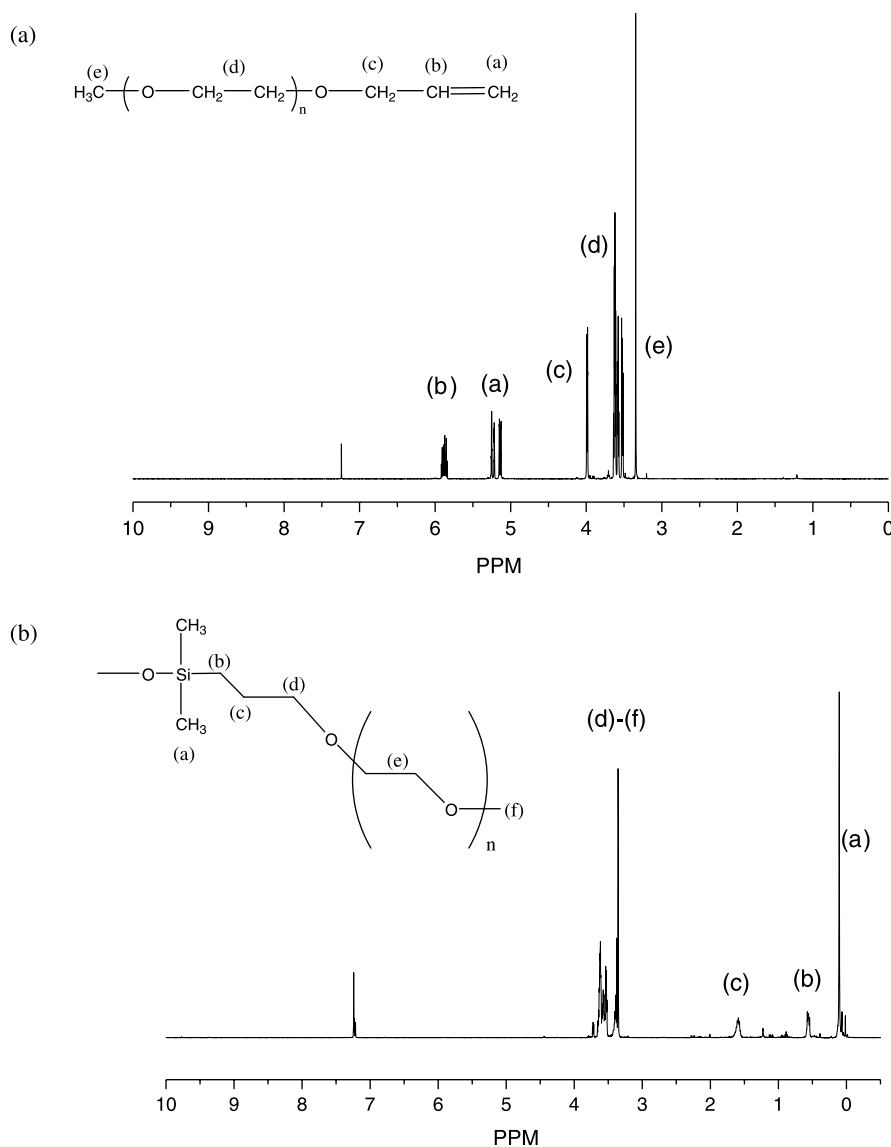


Fig. 1. ¹H NMR spectra of (a) allyl-PEO and (b) PEO-POSS.

FT-IR spectrophotometer in the range $4000\text{--}400\text{ cm}^{-1}$ at a resolution of 1.0 cm^{-1} . All sample preparations were performed under a continuous flow of nitrogen to ensure minimal oxidation or degradation of the sample. Molecular weights were determined by gel-permeation chromatography (GPC) using a SUPER CO-150 apparatus equipped with an LC gel column and an RI detector. Polystyrene samples were used as standards and THF was used as the eluent at a flow rate of 1 mL/min . The thermal and mechanical properties of these hybrids were characterized by thermal gravimetric analysis (TGA) and dynamic mechanical analysis (DMA), respectively. TGA was performed with a TA Instruments TGA 2050 thermogravimetric analyzer at a heating rate of $10\text{ }^\circ\text{C}$ from room temperature to $800\text{ }^\circ\text{C}$ under a continuous flow of nitrogen or air flow. Dynamic mechanical analysis (DMA) measurements were performed using a TA Instruments DMA Q800

(Du Pont) in the tension mode over a temperature range from 30 to $400\text{ }^\circ\text{C}$. Data acquisition and analysis of the storage modulus (E'), loss modulus (E''), and loss tangent ($\tan\delta$) were recorded automatically by the system. A sample was used that was 14 mm in length, 6 mm in width, and 0.2 mm in thickness was used. The heating rate and frequency were fixed at $2\text{ }^\circ\text{C/min}$ and 1 Hz , respectively. The thermal expansion coefficient (TEC) parallel to the surface was measured using a Du Pont TMA 2940 thermomechanical analyzer in extension mode over a temperature range from 25 to $300\text{ }^\circ\text{C}$ with a force of 0.05 N . The dielectric constant and dielectric loss were determined using a Du Pont DEA 2970 dielectric analyzer at a heating rate of $1\text{ }^\circ\text{C/min}$ from 25 to $150\text{ }^\circ\text{C}$ with scan frequencies ranging from 1 to 10^5 Hz . All tests were conducted under a nitrogen flow (20 mL/min) and the specimen thickness was controlled between 0.2 and 0.3 mm .

Table 1
Properties of the PEO–POSS

	M_n	M_w	M_w/M_n	C%	H%	N%
PEO–POSS (theory)	2514 (2938)	2565 (2938)	1.02 (1.00)	42.3 (44.6)	8.01 (7.98)	0.0 (0.0)

Cross-sectional images of the polyimide hybrid films (0.1–0.2 mm) were studied by SEM. The SEM images were obtained using a Hitachi-S4700I microscope operating at an acceleration voltage of 15 kV.

3. Results and discussion

3.1. Synthesis of the PEO–POSS

In this study, we used hydrosilylation reactions to graft allyl-PEO onto the cubic-shaped $Q_8M_8^H$ silsesquioxane, using a modification of previously published procedures [24,25] as shown in Scheme 1. The expected structure can be characterized from 1H NMR spectroscopy, GPC, and elemental analysis (EA). Fig. 1(a) and (b) display the 1H NMR spectra of the allyl-PEO and the PEO–POSS. In Fig. 1(a), the vinyl group of the allyl-PEO is represented by two peaks at 5.2 and 5.9 ppm, in a relative ratio of 2:1; the allylic protons appear as a signal at 3.9 ppm. The protons of the methyl group at the other terminus appear at 3.3 ppm. We assign the peaks at 3.5 and 3.6 ppm to the protons of the repeating $-(CH_2CH_2O)_n-$ units of the PEO. Taking together, this 1H NMR spectroscopic analysis confirms the successful synthesis of allyl-PEO. We prepared the octa-PEO-substituted POSS nanoparticles through the hydrosilylation of allyl-PEO with the $Q_8M_8^H$ POSS generally using 10 equiv. of allyl-PEO per mole of $Q_8M_8^H$; the residual allyl-PEO was removed through evaporation under vacuum or washing with *n*-hexane. In Fig. 1(b), provides evidence for the reactions completion. For example, the protons of the hydrosilane (Si–H) unit at 4.7 ppm, are not present in the

product spectrum. The peak of the methyl units linked to the silicon atoms of $Q_8M_8^H$ appears at 0.1 ppm and new peaks for the $SiCH_2$, $Si-C-CH_2$ protons of PEO–POSS appear at 0.5 and 1.5 ppm, respectively. Thus, this NMR spectrum confirms that our successful synthesis of PEO–POSS occurred exclusively through β -addition without any side reactions occurring during the hydrosilylation process. Table 1 summarizes our results from elemental analysis, and GPC; they are consistent with our NMR spectroscopic analyses. The GPC result in Fig. 2 indicate the very narrow polydispersities of the $Q_8M_8^H$ POSS and PEO–POSS sample, suggest a very uniform molecular weight distribution, with respect to the GPC calibration standards.

3.2. Preparation of the nanoporous polyimide

This nanocomposite approach toward producing polyimide nanofoams usually requires a thermally stable matrix embedded with thermally labile nanoparticles. To obtain a nanoporous polyimide film (Scheme 2), we first coated a soluble polymer precursor onto glass to yield a uniform film, converted it into a phase-separated hybrid upon thermally induced imidization reaction at higher temperatures (usually at 250–300 °C, under an inert atmosphere), and then formed a foam of the film by decomposing the dispersed and thermally labile component at an even-higher temperature (below the T_g). Tables 2 and 3 list thermal properties of the polyimide and its POSS hybrids. We selected the PMDA–ODA polyimide as our matrix because of its high T_g , high thermal stability, and good solubility of the hybrids. Both the PMDA–ODA polyamic acid (PAA) and PEO–POSS are soluble in DMAc prior to thermal

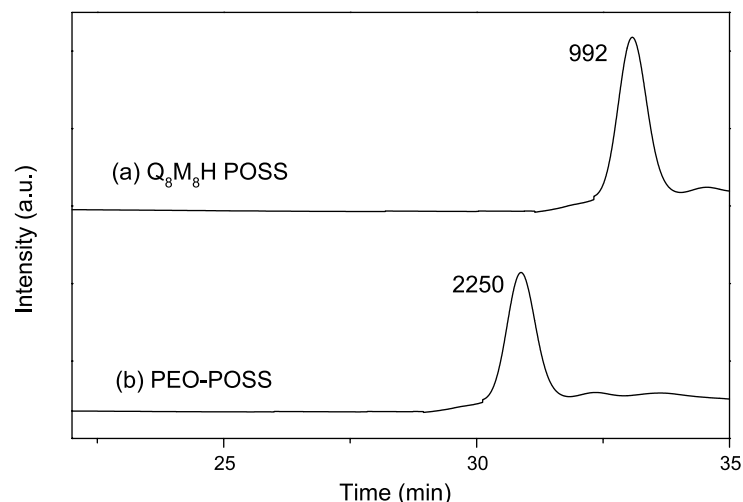
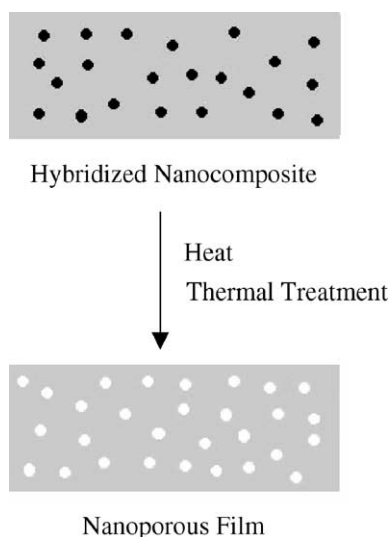


Fig. 2. GPC traces of (a) $Q_8M_8^H$ POSS and (b) PEO–POSS.



Scheme 2. Schematic illustration of the generation of nanoporous polyimide films.

imidization. The labile PEO–POSS undergoes oxidative thermolysis by releasing small molecules as byproducts, which diffuse out of the matrix quantitatively to leave voids in the polymer matrix.

Because the decomposition of the PEO–POSS phase is initiated thermally, it is essential that the PEO–POSS decomposition temperature be below the softening temperature (T_g) of the PMDA–ODA polyimide matrix if we are to prevent collapse of the porous structure [6–8]. The presence of the PEO–POSS phase and the T_g of the PMDA–ODA polyimide hybrid were determined by DMA analysis. The DMA trace (Fig. 3) of the polyimide hybrid containing 10 wt% PEO–POSS displays two transitions, which is characteristic of a micro-phase-separated (>5 nm) morphology. The modulus drop and exhibit a transition at

220 °C may arise from the finite solubility of the PEO–POSS in the matrix or from interfacial relaxation of the PEO and polyimide. The value of T_g of the blended polyimide matrix is ca. 340 °C, which is lower than that observed for the pure polyimide.

After thermal imidization, the foamed hybrid was created by heating the film at 250 °C in air for 12 h. At temperatures below T_g , the labile PEO–POSS phase decomposed and was released from the polyimide leaving voids in the matrix. Because the values of T_g of a cross-linked polyimide is cure-dependent, to obtain a higher softening temperature with this material, it is essential to cure the sample at as high a temperature for decomposition as possible. TGA analyses of PEO–POSS performed under both air and nitrogen indicate (Fig. 4) that the decomposition temperature under oxidative conditions (air) is substantially lower than that obtained under inert atmosphere (N_2). In addition, these TGA analyses indicate the residue of PEO–POSS that remains after heating is silica (SiO_2 ; ca. 38.2 wt%). The PEO–POSS nanoparticles possess sufficient thermal stability at 300 °C under a nitrogen atmosphere to permit material preparation and annealing. Furthermore, the TGA results suggest (Fig. 5) that heating the sample at 250 °C in air is sufficient for quantitative removal of PEO from the hybrid, as shown in Fig. 5. When the hybrid was heated in air, the degradation of PEO–POSS was began at 230 °C and was bimodal, suggesting two competing thermolysis mechanisms for the polyimide/PEO–POSS.

3.3. Dynamic mechanical property of the polyimide hybrids

We obtained detailed information regarding the dynamic mechanical properties of the hybrid films as a function of temperatures. Fig. 6 indicates that the storage modulus and $\tan \delta$, determined through DMA as a function of temperature,

Table 2
Summary of the thermal properties of polyimide nanoporous materials

Sample	PEO–POSS in feed		Softening temperature (°C)	5 wt% loss temperature (°C, in air)	Char yield in air (°C, wt%)
	wt%	mol%			
PI-0P	0	0	370	581	0
PI-2P	2	0.0007	368	578	0
PI-5P	5	0.0017	366	565	3
PI-10P	10	0.0034	360	558	5

Table 3
Summary of the dielectric constant of polyimide nanoporous materials

Sample	PEO–POSS in feed		Dielectric constant (K)	TEC (ppm) 50–250 (°C)	Measured density (g/cm ³)
	wt%	mol%			
PI-0P	0	0	3.25	38.2	1.38
PI-2P	2	0.0007	2.88	42.3	1.31
PI-5P	5	0.0017	2.43	46.5	1.18
PI-10P	10	0.0034	2.25	55.8	1.09

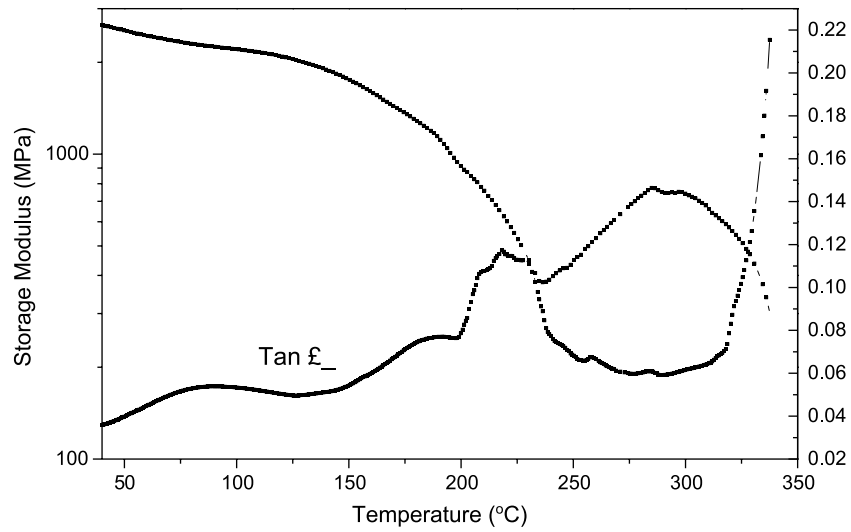


Fig. 3. DMA curves for the polyimide hybrid containing 10 wt% PEO-POSS content recorded at a heating rate of 2 °C/min.

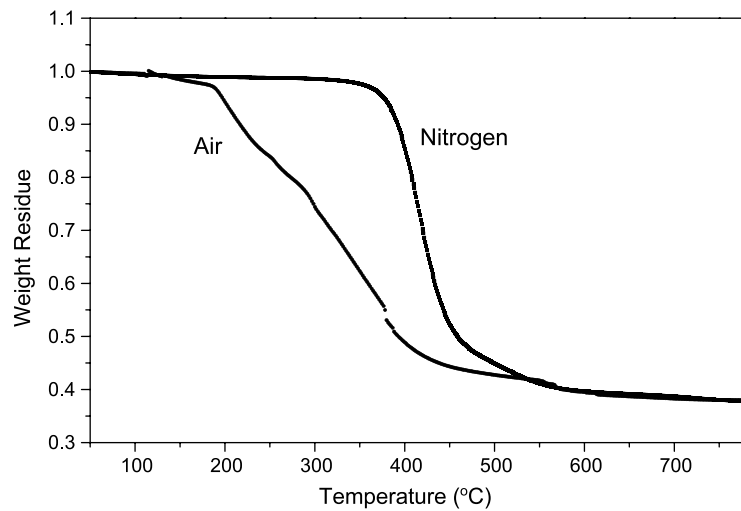


Fig. 4. TGA thermograms of the PEO-POSS recorded in air and nitrogen.

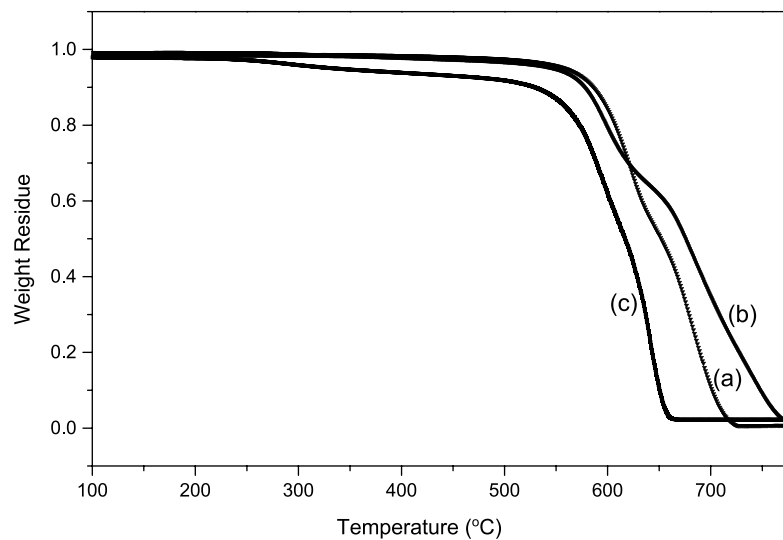


Fig. 5. TGA thermograms of (a) the pure polyimide, (b) the porous polyimide containing 10 wt% PEO-POSS content after foaming and (c) the polyimide hybrid containing 10 wt% PEO-POSS content prior to foaming.

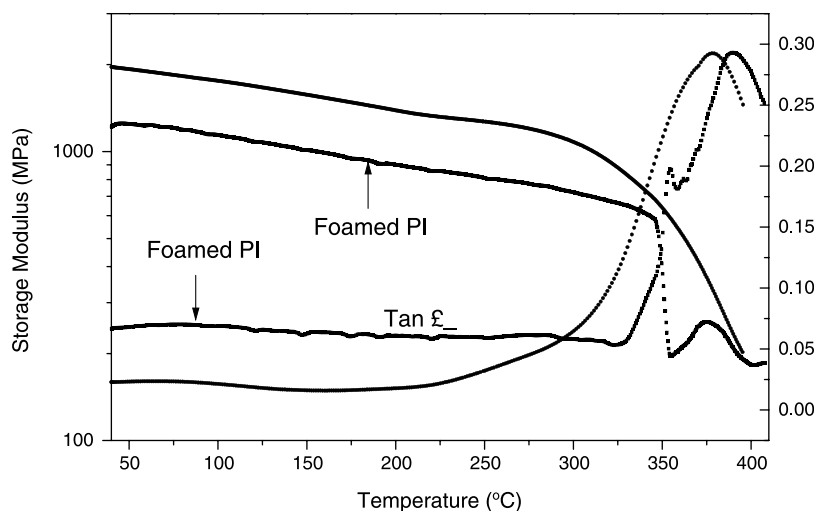


Fig. 6. DMA curves for the pure and porous polyimide (obtained from 10 wt% PEO–POSS) recorded at a heating rate of 2 °C/min.

of the pure and porous polyimides prepared from 5 to 10 wt% PEO–POSS. Pure polyimide has a modulus of ca. 2000 MPa at room temperature and a single value of T_g (370 °C). In the case of the porous polyimide, two relaxations appear at ca. 360 and 385 °C based on the $\tan \delta$ peaks. The relaxation at 360 °C is a typical microphase separation for the porous polyimide along with a sudden decrease in storage modulus. Such a transition (360 °C cf. 370 °C for the homopolymer) results from the finite solubility of the PEO–POSS nanoparticles in the matrix and the microphase separation of the foams after curing. The overall modulus of the porous polyimide is lower than that of the pure polyimide, again most likely due to the foaming structure. At higher temperatures (>370 °C), these foams collapsed and the porous structure was no longer present. The observed higher T_g of the nanoporous system (385 °C based on the maximum of the $\tan \delta$ peak) is probably due to the content of residual

silica produced by PEO–POSS in the solid matrix. It is clear that the storage modulus and softening temperature (T_g) decrease slightly with increasing content of nanofoam in the polyimide matrix. Fig. 7 displays the DMA spectra of the pure polyimide, 5 and 10 wt% PEO–POSS nanocomposites of polyimide in comparison with the foamed polymer sample obtained after post-curing at 400 °C for 2 h. After post-curing, these foams were collapsed and their storage modulus was increased upon increasing their PEO–POSS contents. In addition, the relaxation from the microphase separation of the nanofoams was disappeared. The increased modulus in this nanocomposite may arise from the SiO₂ particles from the PEO–POSS that are distributed evenly within the polymer matrix on a nanometer scale. The result may come from the physical bond such as hydrogen bonding interactions between the polyimide and these rigid silica particles would hinder the mobility of the polymer chains,

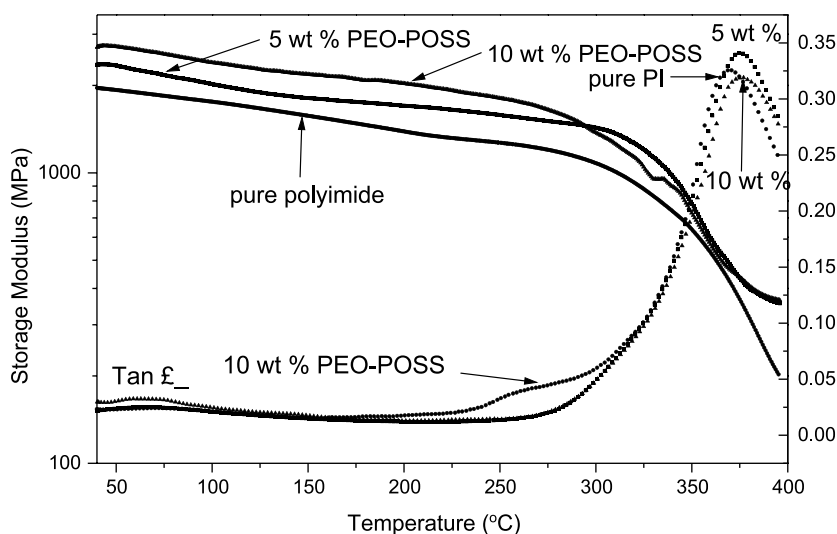


Fig. 7. DMA curves recorded at a heating rate of 2 °C/min for the pure polyimide and those containing various PEO–POSS contents after annealing at 400 °C.

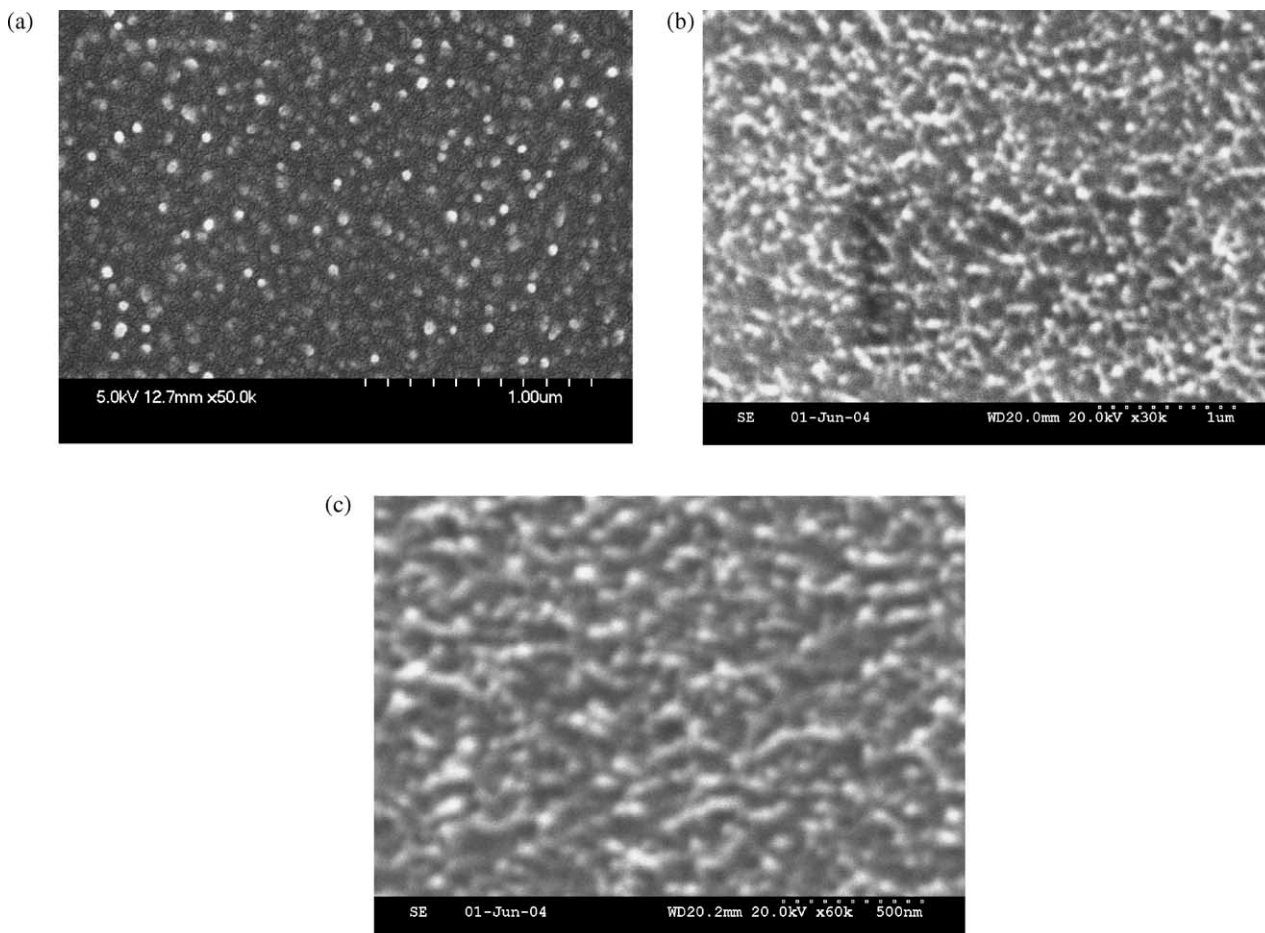


Fig. 8. SEM cross-section images of PI-POSS hybrid materials containing (a) 5 wt% PEO-POSS content recorded prior to foaming, (b) 5 wt% and (c) 10 wt% PEO-POSS content recorded after foaming.

which results in their higher-than-expected modulus and value of T_g .

3.4. Dielectric properties

Recently, lower dielectric constants are one of the most desirable properties of next-generation electronic devices [26,27]. Table 3 gives the dielectric constants of the various composites having different POSS contents. The dielectric constant of the hybrid was decreased upon increasing the POSS content. The measured dielectric constant of the pure polyimide is 3.25 (1 MHz); the lowest dielectric constant was observed for this series of the porous polyimides was 2.25 for the sample incorporating of 10 wt% PEO-POSS. The reduction in the dielectric constant of the polyimide hybrids can be explained in terms of the foam's porous structure creating loose polyimide morphology. The void formation and the free volume increase of the polyimide nanocomposite can be qualitatively verified qualitatively by measuring its density [28,29]. The density of the pure polyimide is 1.38 while that of the nanocomposite containing 10 wt% POSS is 1.09. Scheme 2 shows the loose polyimide structure that forms in the nanofoams. The

increase in the free volume of the polyimide corresponds quite well to the decrease of the modulus (E') and the glass transition temperature (T_g) of the porous polyimide.

3.5. SEM analysis

Fig. 8(a) displays a cross-sectional SEM image of the polyimide hybrid film containing 5 wt% PEO-POSS prior to its foaming. We observe a uniform distribution of PEO-POSS nanoparticles of 20 nm size within the polyimide matrix. Fig. 8(b) presents an SEM image of the porous structure prepared from the 5 wt% PEO-POSS sample after performing its foaming process. The observed porous structures are less spherical (dimensions: 10–40 nm), possess a small degree of interconnection, and are slightly deviated from their pre-foaming morphology. The reason for this deviation from the expected spherical morphology is due to the foaming process. These small molecules created from the thermal decomposed PEO-POSS nanoparticles escape from the PI matrix; this process tends to change the pore's original spherical shapes and sizes and causes certain pore interconnections to form. At a certain point, however, molecular motion of the polymer chain decreases and the film

is frozen into non-equilibrium morphology [30]. Fig. 8(c) shows the morphology of the hybrid containing 10 wt% PEO–POSS; the pore sizes in this sample have become larger and there is a greater degree of pore interconnection.

4. Conclusions

We have successfully synthesized a PEO-functionalized POSS (PEO–POSS) possessing a silsesquioxane unit at its core. Incorporation of oligomeric PEO chains onto the silsesquioxane core significantly reduced PEO–POSS self-aggregation and enhances its solubility in the polyamic acid matrix prior to imidization. To obtain nanoporous polyimide films, we coated the soluble precursor polymers onto a glass plate to yield uniform films, converted them into phase-separated hybrids through imidization, and then foamed them upon decomposition of the thermally labile PEO–POSS moieties. The PMDA–ODA polyimide/PEO–POSS hybrids were prepared at 300 °C under nitrogen and transformed into a porous structure by annealing at 280 °C in air. SEM analysis indicated that the PEO–POSS units were micro-phase-separated in the polyimide matrix with domain sizes of 20 nm. We generated the final nanoporous (10–40 nm) hybrids from these films through a foaming process. In so doing, we managed to lower the bulk dielectric constant of the thin film from 3.25 to 2.25 was accomplished. These porous materials exhibit high thermal stability and good mechanical strength and are strong candidate for use as the next-generation low-*k* materials.

References

- [1] Bohr MT. Tech Digest IEEE Int Electron Devices Meeting 1995;241.
- [2] Edelstein DC, Sai-Halasz GA, Mi YJ. IBM J Res Dev 1995;39:83.
- [3] Wilson SR, Tracy CJ. Handbook of multilevel metallization for integrated circuits. Park Ridge, NJ, USA: Noyes Publications; 1993.
- [4] National Technology Roadmap for Semiconductors: Semiconductor Industry Association; 1997.
- [5] National Technology Roadmap for Semiconductors: Semiconductor Industry Association; 1999.
- [6] Carter KR, McGrath JE. Chem Mater 1997;9:105.
- [7] Carter KR, DiPietro RA, Sanchez MI, Swanson SA. Chem Mater 2001;13:213.
- [8] Mikoshiba S, Hayase S. J Mater Chem 1999;9:591.
- [9] Krause BR, Mettinkhof NF. Macromolecules 2001;34:874.
- [10] Krause BR, Mettinkhof NF. Adv Mater 2002;14:1041.
- [11] Gross J, Reichenauer G, Fricke J. J Phys D: Appl Phys 1988;21:1447.
- [12] Gross J, Fricke J. J Non-Cryst Solids 1992;145:217.
- [13] Licata TJ, Colgan EG, Harper ME, Luce SE. IBM J Res Dev 1995;39:419.
- [14] Murarka S. Solid State Technol 1996;39:83.
- [15] Hougham G, Tesoro G, Viehbeck A, Chapple-Sokol JD. Macromolecules 1994;27:5964.
- [16] Bergman DJ, Stroud D. J Phys, Solid State Phys 1992;46:147.
- [17] Cha HJ, Hedrick JL, Dipietro RA, Blume T, Beyers R, Yoon DY. Appl Phys Lett 1996;68:1930.
- [18] Azzam RMA, Bashara NM. Ellipsometry and polarized light. Amsterdam: Elsevier; 1977.
- [19] Sellinger A, Laine RM. Macromolecules 1996;29:2327.
- [20] Lichtenhan JD, Otonari YA, Carr MJ. Macromolecules 1995;28:8435.
- [21] Zheng L, Farris RJ. J Polym Sci, Polym Chem Ed 2001;39:2920.
- [22] Andre L, Lichtenhan JD. Macromolecules 1998;31:4970.
- [23] Haddad TS, Lichtenhan JD. Macromolecules 1996;29:7302.
- [24] Lestel L, Cheradame H, Boileau S. Polymer 1990;31:1154.
- [25] Prithwiraj M, Wunder SL. Chem Mater 2002;14:4494.
- [26] Zhang YH, Dang ZM, Fu SY, Xin JH, Deng JG, Wu J, et al. Chem Phys Lett 2005;401:553.
- [27] Zhang YH, Lu SG, Li YQ, Dang ZM, Xin JH, Fu SY, et al. Adv Mater 2005;17:1056.
- [28] Leu CM, Chang YT, Wei KH. Macromolecules 2003;36:9122.
- [29] Leu CM, Chang YT, Wei KH. Chem Mater 2003;15:3721.
- [30] Briber RM, Fodor JS, Russell TP, Miller RD, Hedrick JK. Mater Res Soc Symp Proc 1997;461:272.